

## DFT / TDDFT insights into excited state intra-molecular hydrogen atom transfer mechanism in Liqcoumarin: an EFP1 study

Kandigowda JAGADEESHA\* , Yelechakanahalli Lingaraju RAMU , Mariyappa RAMEGOWDA 

Department of Physics, Government College, Mandya, India

Received: 28.08.2021

Accepted/Published Online: 25.10.2021

Final Version: 23.02.2022

**Abstract:** The theoretical calculations were carried out on Liqcoumarin (LC) and its water complex  $LC+(H_2O)_4$ -[LCH] at the ground ( $S_0$ ) / first excited states ( $S_1$ ) by employing density functional theory (DFT) / state specific time-dependent density functional theory (SS-TDDFT). In LC and LCH, there is an intra-molecular hydrogen bond between hydroxyl group and acetyl group along with four inter-molecular hydrogen bonds in the hydrated molecule. The computational studies of molecular structural parameters, electrostatic potential, NBO analysis, molecular orbital's, and UV-Vis spectra of both molecules under polar solvents were explored by B3LYP / 6-31G (d,p) / PCM / EFP1 method. The intra-molecular hydrogen atom transpires between hydroxyl to acetyl group in both pure and hydrated molecules confirm the ICT process, and it affirms through potential energy surface (PES) scans.

**Key words:** Liqcoumarin, hydrated liqcoumarin, density functional theory, time dependent density functional theory, effective fragment potential

### 1. Introduction

The phenomenon of hydrogen bonding has been illustrious for its eminence in various fields like photophysics, photochemistry, and biochemistry. The systematic study of hydrogen bonds is much essential for comprehending the photo-physical properties of some organic molecules, which is having electron donor and acceptor demeanor at both ground and excited states [1–4]. The EFP method furnishes a polarizable QM-based force field to characterize the inter-molecular interactions. To study the microsolvation effect on biological or organic molecule, EFP1 / DFT method was established explicitly for solvation, and it interfaced with the polarizable continuum model (PCM) [5,6], and also EFP1 / TDDFT method has been fostered for characterizing the electronically excited states of solvated molecules [5, 7–9]. In order to enlighten the electronic, molecular, structural, and photo-physical properties of many organic and biological molecules, TDDFT computations are done at excited states. At the excited state, there is a refashioning in the molecular structure, which takes place within the molecule along with hydrogen transfer. The revamp of hydrogen bond anatomy due to microsolvation effect is to evince the ESIPT / ESIHT process in some organic and biological molecules. The intra-molecular charge transfer character correlated with ESIPT / ESIHT is associated to the photophysical features of biologically active molecules [10].

The naturally occurring herb *Glycyrrhiza glabra* (Licorice) is one of the most widely used herbs, which exhibits a broad range of biological activities both in traditional medicine and flavouring, belonging to the Leguminosae (Fabaceae) family [11,12]. The roots of *Glycyrrhiza glabra* gave more than 400 compounds, and the main phenols identified from the root are isoliquiritin, liquiritin, and coumarins, including umbelliferone, Liqcoumarin (LC), glabro coumarone A and B [13–15]. Pharmacological studies have confirmed that biologically active compounds in *Glycyrrhiza* plant exhibit a broad range of biological activities like anti-diabetic [16], anti-microbial [17], anti-carcinogenic [18], anti-oxidant [19], cytotoxic, anti-tumor [20], anti-inflammatory [21,22], anti-viral [23]. A series of compounds synthesized from 6-coumarin derivatives showed potent inhibitory activity against human immunodeficiency virus (HIV-1) infection with  $IC_{50}$  [24]. The  $\alpha$ -pyrano chalcones [Gb1–Gb2], which were synthesized from 6-acetyl-5-hydroxy-4-methyl-2H-chromen-2-one exhibits anti-malarial activity against *P. Falciparum* such that halogenated derivatives (Gb1) exhibited greater activity than the methoxylated derivative (Gb2) [25]. LC is one of the hydroxycoumarin having 26 atoms in which methyl (-CH<sub>3</sub>), hydroxyl (-OH), and acetyl groups are attached to the C4, C5, and C6 positions of basic coumarin moiety. LC has an intra-molecular hydrogen bond between hydroxyl group and acetyl group and can also form four inter-molecular hydrogen bonds with

\* Correspondence: jageethasha.physics@gmail.com

four solvent molecules. In the present theoretical study, the DFT / TDDFT / EFP1 methods were used to investigate LC and LCH molecules in the ground and excited states and also the electronic structure; ICT states of the molecules along with the ESHT process have been explored.

## 2. Computational methods

Avogadro[26] is an advanced molecule editor and visualizer employed to design the pure molecule and its water complex, LCH, optimized at equilibrium geometry using MMFF94s force field [27]. All theoretical computations were executed by GAMESS-US software suite [28,29]. The gas phase geometry optimization of LC and LCH molecules at both ground state ( $S_0$ ) and first excited state ( $S_1$ ) was carried out without symmetry constraints using 6-31G(d,p) basis set [30]. This procedure was considered satisfactory if the energy difference between optimized cycles was  $(3-6) \times 10^{-5}$  Hartree / Bohr and a gradient of  $<1 \times 10^{-5}$  Hartree/Bohr was achieved. Computational methods like DFT [31-36] / SS-TDDFT [37,38] are the attractive and useful tools to generate the gas phase optimized molecular geometries of LC and LCH both at  $S_0$  and  $S_1$  states by using hybrid functional B3LYP [39,40] with 6-31G(d,p) basis set. The natural charges on various atoms and groups of both molecules at ground and excited states were computed using NBO.6 program [41]. The Frontier molecular orbitals and MEP maps are plotted by wxMacMolPlt[42], which is an open-source application for visualization.

## 3. Results and discussion

### 3.1. Electronic structural studies at $S_0$ and $S_1$ states

The gas phase optimized geometrical parameters of LC and LCH molecules at  $S_0$  and  $S_1$  states namely bond lengths, bond angles are computed by DFT / TDDFT / B3LYP / 6-31G(d,p) levels. At ground state of LC and LCH molecules, the intra-molecular HB O15-H23.....O16=C11 exist between hydroxy group and acetyl group and it modified as O16-H23.....O15=C1 at the first excited state. Four inter-molecular hydrogen bonds exist between the pure molecule and solvated water molecules; two HB's will exist between oxygen of hydroxyl group and oxygen of carbonyl group and another two HB's will exist across the keto group of pyrone ring. One hydrogen bond exists between micro-solvated water molecules across the hydroxyl group and oxygen of the carbonyl group.

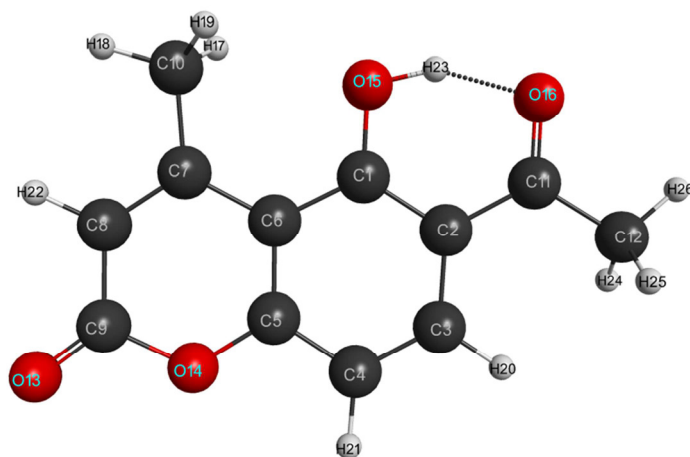
When pure molecule LC undergo photo-excitation, the bond lengths C1-C2 / C3-C4 / C5-C6 / C7=C8 / C1-C6 increased by 0.026 / 0.044 / 0.053 / 0.032 / 0.034 Å and C2-C3 / C4=C5 / C6-C7 / C11-C12 / C2-C11 decreased by 0.021 / 0.038 / 0.044 / 0.024 / 0.019 Å. In the pyrone ring, bond lengths C9=O13 / C5-O14 increases by 0.01 / 0.011 Å, whereas bond length C9-O14 decreased by 0.022 Å. Due to hydrogen atom transfer (H23) from hydroxyl group to the carbonyl group, C1-O15 becomes C1=O15, and its bond length decreased by 0.058 Å; C11=O16 becomes C11-O16, and its bond length increased by 0.086 Å. The bond lengths of C-H combinations in the LC molecule decreased / increased in the range of  $(1-5) \times 10^{-3}$  Å. The bond angles between different atoms vary from  $0.1^\circ$  to  $4.6^\circ$ .

Due to the effect of micro-solvation, the optimized geometrical parameters of LCH molecule changes. The bond lengths C3-C4 / C7=C8 / C7-C10 / C2-C11 / C1-O15 increased by 0.004 / 0.002 Å / 0.001 / 0.006 / 0.01 Å and C1-C2 / C2-C3 / C4-C5 / C5-C6 / C6-C7 / C8-C9 / C11-C12 / C11-C16 / C1=C6 decreased by 0.007 / 0.005 / 0.005 / 0.001 / 0.002 / 0.005 / 0.008 / 0.002 / 0.001  $\times 10^{-2}$  Å. In the pyrone ring, bond lengths C9=O13 / C5-O14 / C1=O15 / O15-H23 increased by 0.011 / 0.008 / 0.01 / 0.012 Å, whereas bond length C9-O14 / C11-O16 decreases by 0.014 / 0.002 Å. The bond lengths of C-H combinations in the LCH molecule decreased / increased in the range of  $(0-6) \times 10^{-3}$  Å. The bond angles between the respective atoms varies from  $0^\circ$  to  $1.3^\circ$ .

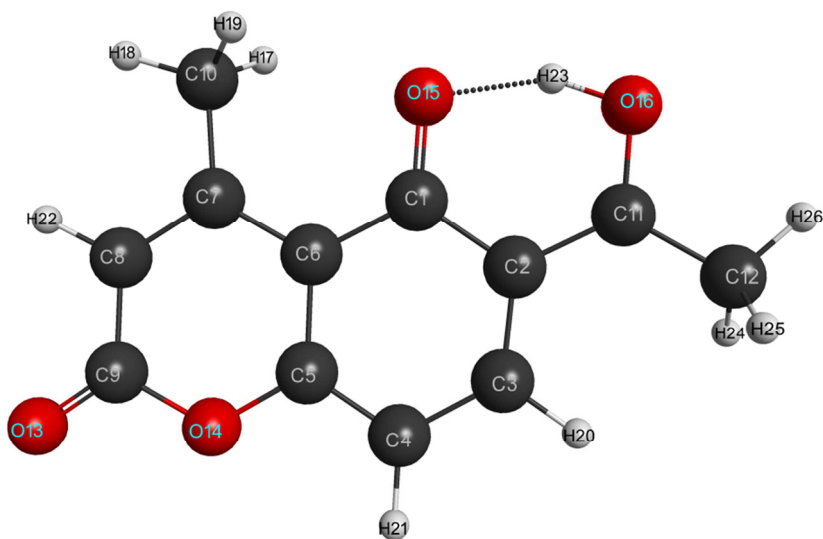
When microsolvated molecule LCH undergo excitation, the bond lengths C1-C2 / C3-C4 / C5-C6 / C7=C8 / C1=C6 increased by 0.029 / 0.043 / 0.049 / 0.0321 / 0.034 Å and C2-C3 / C4=C5 / C6-C7 / C11-C12 / C2-C11 decreased by 0.018 / 0.036 / 0.04 / 0.019 / 0.02 Å. In the pyrone ring, bond lengths C9=O13 / C5-O14 increases by 0.004 / 0.01 Å, whereas bond length C9-O14 decreased by 0.015 Å. Due to hydrogen atom transfer (H23) from hydroxyl group to carbonyl group, C1-O15 becomes C1=O15, and its bond length decreased by 0.061 Å; C11=O16 becomes C11-O16, and its bond length increased by 0.092 Å. The bond lengths of C-H combinations in the LC molecule decreased / increased in the range of  $(1-6) \times 10^{-3}$  Å. The bond angles between different atoms vary from  $0.1^\circ$  to  $3.8^\circ$ . The optimized equilibrium structures of LC and LCH molecules at  $S_0$  and  $S_1$  states with an atom numbering scheme are shown in Figures 1,2. The structural parameters like bond lengths, bond angles at  $S_0$  and  $S_1$  states are summarized in Tables 1,2.

### 3.2. Simulation of UV-Vis spectra

To our knowledge, theoretical studies on LCH have been performed so far to study its interaction in water and methanol solvents. It is observed that, the bond lengths, bond angles, dihedral angles of LC and LCH molecules change appreciably, and also excitation energy in the first excited state changes due to the non-covalent bonding interaction between LC and LCH with polar solvents, i.e. the first excitation energy of LC and LCH molecules corresponding to methanol and water



(a)



(b)

**Figure 1.** Optimized equilibrium molecular structures of LC molecule at (a)  $S_0$  and (b)  $S_1$  state.

solvents as 3.788 eV / 3.872eV, 3.789eV / 3.871eV, while the excitation energy of LC and LCH molecules in the gas phase is 3.756eV / 3.901eV.

The electronic transitions that occur in the pure and micro solvated molecules LC and LCH are identified by UV-Vis spectral analysis. By using TDDFT / PCM / B3LYP / 6-31G (d, p) method, the theoretical electronic absorption spectral wavelengths of LC and LCH molecules in the gas phase / water / methanol exhibit an intense band near 330 / 327.2 / 327.3nm, and 317.8 / 320.29 / 320.21nm, respectively. The calculated electronic absorption spectra of LC and LCH in the gas phase and in various polar protic solvents using the polarizable continuum model (PCM) are presented in Figure 3. The locality of absorption bands is regulated by water and methanol solvents. The vertical absorption energies, oscillator strengths, and probable wave functions are depicted in Table 3 evinces solvent effects on the electronic  $\pi \rightarrow \pi^*$  transitions states of LC and LCH molecules, i.e. in polar solvents; the energies of the  $\pi \rightarrow \pi^*$  electronic transitions are increased and thereby decrease in absorption wavelength; the UV-Vis spectra signalize a systematical blue shift in LCH, and the

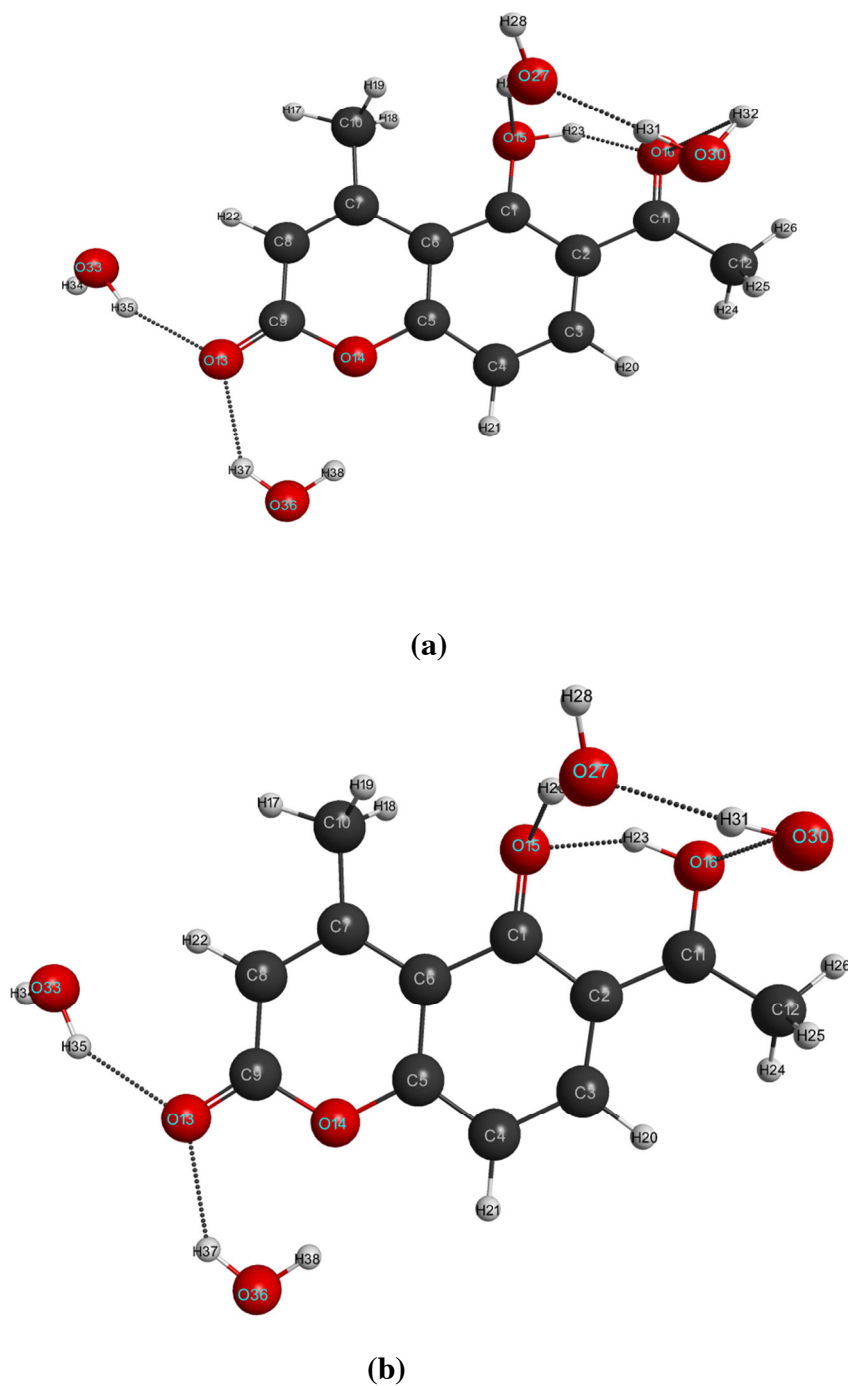


**Figure 2.** Optimized equilibrium molecular structures of LCH molecule at (a)  $S_0$  and (b)  $S_1$  state.

calculated absorption wavelength difference corresponds to 12.2nm, 6.91nm, and 7.09nm respectively, while moving from gas to methanol solvents. The theoretical absorption spectral wavelength of pure LC in methanol solvent was about 327.3 nm, which is approximately consistent with experimental value, which is about 310nm [43].

### 3.3. Molecular orbitals

The frontier molecular orbitals are discussed for both LC and LCH molecular systems. HOMO, HOMO-1, LUMO and LUMO+1 energies were computed by TD-DFT / B3LYP / 6-31G(d,p) method and are picturized in Figures 4,5. The

**Table 1.** Selected bond lengths of LC and LCH molecules at  $S_0$  and  $S_1$  states.

r(Å)	LC-S0	LC-S1	LCH-S0	LCH-S1
C1-C2	1.426	1.452	1.419	1.448
C2-C3	1.413	1.392	1.408	1.39
C3-C4	1.376	1.42	1.38	1.423
C4-C5	1.405	1.367	1.4	1.364
C5-C6	1.411	1.464	1.41	1.459
C6-C7	1.461	1.417	1.459	1.419
C7-C8	1.361	1.393	1.363	1.394
C8-C9	1.447	1.441	1.442	1.441
C9-O13	1.207	1.216	1.218	1.222
C5-O14	1.353	1.364	1.361	1.371
C9-O14	1.406	1.384	1.392	1.377
C7-C10	1.506	1.502	1.507	1.502
C8-H22	1.084	1.083	1.083	1.082
C10-H17	1.094	1.093	1.092	1.092
C10-H18	1.092	1.093	1.093	1.092
C10-H19	1.093	1.093	1.094	1.094
C12-H24	1.095	1.099	1.095	1.097
C12-H25	1.096	1.101	1.094	1.1
C12-H26	1.09	1.092	1.09	1.092
C11-C12	1.514	1.49	1.506	1.487
C2-C11	1.466	1.447	1.472	1.452
C11-O16	1.246	1.332	1.244	1.336
C1-O15	1.332	1.274	1.342	1.281
C15-H23	1.007	1.016	1.019	1.008
C1-C6	1.425	1.459	1.424	1.458

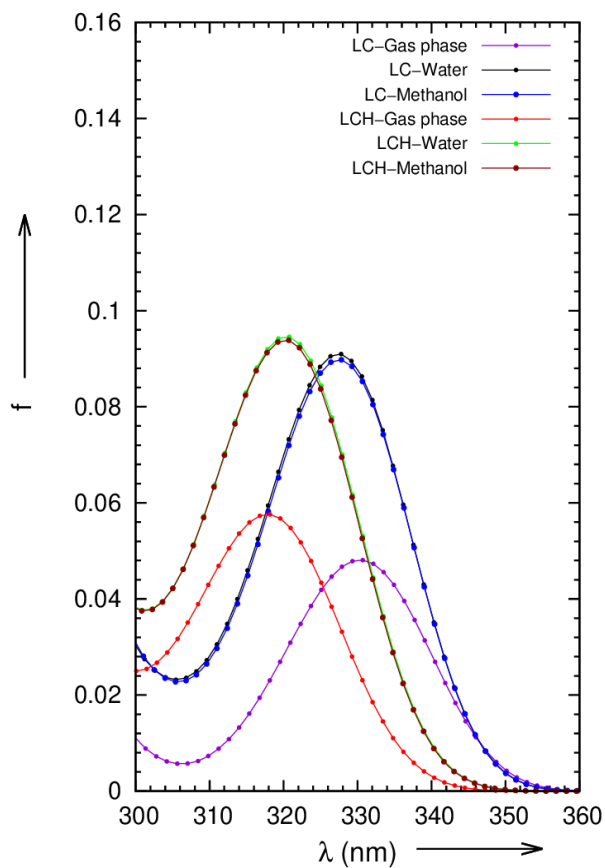
LUMO+1, LUMO, HOMO and HOMO-1 energies corresponds to LC / LCH molecules are  $-1.5782\text{eV}$  /  $-1.8775\text{eV}$ ,  $-1.9592\text{eV}$  /  $-2.0952\text{eV}$ ,  $-6.3402\text{eV}$  /  $-6.6395\text{eV}$  and  $-6.6667\text{eV}$  /  $6.9933\text{eV}$ . The energy gap between (HOMO-LUMO), (HOMO-1-LUMO+1) explains the eventual charge transfer reactions occur within the LC / LCH molecules, which are given by  $4.381\text{eV}$ ,  $5.088\text{eV}$  /  $4.5443\text{eV}$ ,  $5.11158\text{eV}$ . It is observed that, the energy difference between (HOMO-LUMO) and (HOMO-1-LUMO+1) increases in LCH due to the effect of microsolvation.

### 3.4. Natural charge analysis

The NBO 6.0 calculations were carried out at both ground and first excited states of LC and LCH using computational package like GAMESS integrated with NBO 6.0 program at DFT / TDDFT / B3LYP / 6-31G(d, p) level. It provides a convenient basis for investigating charge transfer mechanism in LC and LCH molecules at first excited state. The charge analysis rendered on the electronic structure of LC and LCH molecules precisely describes the allocation of electrons in different sub shells of their AOs. The natural charges on various atoms of LC and LCH molecules at ground and excited states are tabulated in Table 4. The natural charges on O15 / O16 / H23 atoms becomes  $-0.694\text{e}$  /  $-0.601\text{e}$  /  $0.527\text{e}$  and  $-0.736\text{e}$  /  $-0.614\text{e}$  /  $0.527\text{e}$ , respectively in the ground state of LC and LCH molecules. The total natural charge of acetyl / hydroxyl group (O15-H23) / methyl groups / benzene ring / pyrone rings becomes  $0.015\text{e}$  /  $-0.167\text{e}$  /  $0.073\text{e}$  /  $0.435\text{e}$  /  $-0.115\text{e}$  and  $0.039\text{e}$  /  $-0.209\text{e}$  /  $0.07\text{e}$  /  $0.465\text{e}$  /  $-0.157\text{e}$  in the ground state of LC and LCH molecules, respectively. The natural charge on O15 / O16 / acetyl group / hydroxyl group / benzene ring / pyrone ring increased by  $-0.042\text{e}$  /  $-0.012\text{e}$  /  $0.048\text{e}$  /  $0.054\text{e}$  /  $0.030\text{e}$  /  $-0.042\text{e}$ , where as natural charge on H23 / methyl group decreased by  $0.0005\text{e}$  /  $0.0027\text{e}$  due to effect of micro-solvation.

**Table 2.** Selected bond angles - A(°) of LC and LCH molecules at S<sub>0</sub> and S<sub>1</sub> states.

A(°)	LC-S0	LC-S1	LCH-S0	LCH-S1
C1-C2-C3	119.0	118.5	119.0	118.2
C2-C3-C4	121.5	124.4	121.5	124.3
C3-C4-C5	119.0	118.4	118.7	118.4
C4-C5-C6	123.0	121.4	123.2	121.5
C5-C6-C7	117.0	118.0	117.7	118.0
C6-C7-C8	118.3	118.2	118.6	118.5
C7-C8-C9	124.0	123.6	123.2	123.0
C8-C9-O14	115.2	117.0	116.2	117.6
C9-O14-C5	122.8	121.8	122.7	121.7
O14-C5-C6	122.0	121.5	121.5	121.4
C1-O15-H23	106.0	101.4	104.7	100.9
C2-C1-O15	120.0	120.7	119.8	120.7
C2-C11-O16	121.0	120.3	120.4	120.0
C1-C2-C11	119.0	119.6	119.0	120.0
C12-C11-O16	118.4	115.6	119.1	115.4
C6-C1-O15	119.0	121.1	119.2	120.6

**Figure 3.** Simulated absorption spectra of LC and LCH molecules in gas phase, water and methanol solvents.

**Table 3.** Peaks represents the theoretical simulated UV-Vis absorption wavelengths ( $\lambda$ ) of LC and LCH molecules corresponds to electronic transition  $S_0 \rightarrow S_1$  with oscillator strengths (f) in gas phase, water and methanol solvents.

Molecule	Solvent / gas phase	$\lambda_a$ (nm)	f	Wave function (excitation amplitude)
LC	Gas phase	330.0	0.0557	H $\rightarrow$ L(-0.916), H-1 $\rightarrow$ L(-0.141), H-1 $\rightarrow$ L+1(-0.118) H $\rightarrow$ L+1(0.332), H-1 $\rightarrow$ L+2(-0.130)
	Water	327.2	0.1065	H $\rightarrow$ L(-0.941), H-1 $\rightarrow$ L(-0.130), H-1 $\rightarrow$ L+1(-0.104) H $\rightarrow$ L+1(0.268), H-1 $\rightarrow$ L+2(-0.120)
	Methanol	327.3	0.1053	H $\rightarrow$ L(0.943), H-1 $\rightarrow$ L(0.127), H-1 $\rightarrow$ L+1(0.103) H $\rightarrow$ L+1(-0.263), H-1 $\rightarrow$ L+2(0.118)
LCH	Gas phase	317.8	0.0685	H $\rightarrow$ L(0.903), H-1 $\rightarrow$ L(0.158), H-1 $\rightarrow$ L+1(-0.102) H $\rightarrow$ L+1(0.360), H-1 $\rightarrow$ L+2(0.138)
	Water	320.29	0.1139	H $\rightarrow$ L(0.937), H-1 $\rightarrow$ L(-0.139), H-1 $\rightarrow$ L+1(-0.098) H $\rightarrow$ L+1(-0.279), H-1 $\rightarrow$ L+2(-0.123)
	Methanol	320.21	0.1130	H $\rightarrow$ L(-0.937), H-1 $\rightarrow$ L(0.138), H-1 $\rightarrow$ L+1(0.096) H $\rightarrow$ L+1(0.280), H-1 $\rightarrow$ L+2(0.123)

When LC and LCH molecules undergo photo-excitation, the natural charges on O15 / O16 / H23 atoms become  $-0.667e / -0.666e / 0.523e$  and  $-0.716e / -0.684e / 0.528e$  respectively. The total natural charge of methyl group / benzene ring / pyrone rings becomes  $0.094e / 0.484e / 0.059e$  and  $0.096e / 0.532e / 0.032e$  in LC and LCH, respectively. The natural charge on O16 / methyl group / benzene ring / pyrone ring increased by  $-0.065e / -0.021e / 0.049e / 0.173e$ ,  $-0.07e / 0.026e / 0.067e / 0.189e$ , whereas natural charge on O15 / H23 decreased by  $-0.027e / 0.004e$ ,  $-0.020e / 0.005e$  in the first excited state of LC and LCH molecules. In LC molecule, the charge on O15 / H23 decreased by  $0.027e / 0.004e$ , and the charge on O16 increased by  $0.065e$ . Whereas, in LCH molecule, the charge on O15 / H23 decreased by  $-0.02e / 0.005e$ , and the charge on O16 increased by  $0.07e$ . So, an intra-molecular hydrogen atom (H23) transfer takes place from hydroxyl group (O15-H23) to carbonyl group (C11-O16), i.e. ICT takes place both in LC and LCH molecules in the excited state.

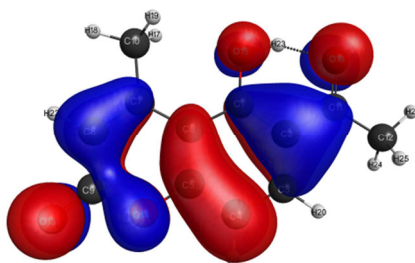
### 3.5. Molecular electrostatic potential (MEP)

The 3D plot of total electron density called MEP is enlightened to predict reactive sites for the LC and LCH molecules by employing the optimized geometry parameters at 6-31G(d,p) / B3LYP / DFT level. MEP can be a substantial presentation for the elucidation of non-covalent interactions, aggression of electrophilic and nucleophilic at appropriate zone of the investigated system. The magnitude of the electrostatic potential at the LC and LCH are expressed by benchmark colors, i.e. red, blue and green colors displays the most negative, positive, and zero electrostatic potential. From MEP of LC and LCH molecules at the ground and first excited states, the dark red colored zone over the oxygen atoms delineates electrophilic (electron rich) reactivity, and the dark blue coloured zone over the hydrogen atoms delineates the nucleophilic (electron deficient) reactivity, i.e. the sites insinuating the negative electrostatic potential are focalized at the conjugated aromatic rings, whereas the sites insinuating the positive potential are focalized at the aromatic hydrogen atoms. The MEP plots with charges on various atoms and groups of LC and LCH molecules at ground and first excited states are portrayed in Figures 6,7.

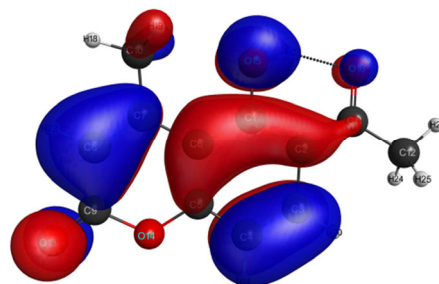
### 3.6. Hydrogen bond (HB) dynamics

To depict the comprehensive perspectives of both intra-molecular and inter-molecular hydrogen bonds at ground state and first excited states, theoretical study have been effectuated on pure molecule and its water complex at DFT / TDDFT

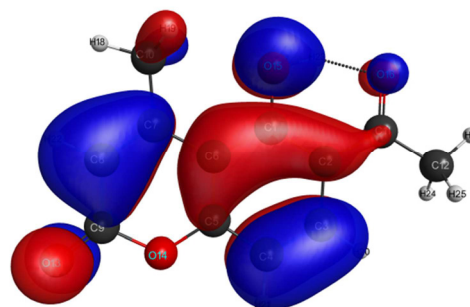
**Homo-1**



**Homo**



**Lumo**



**Lumo+1**

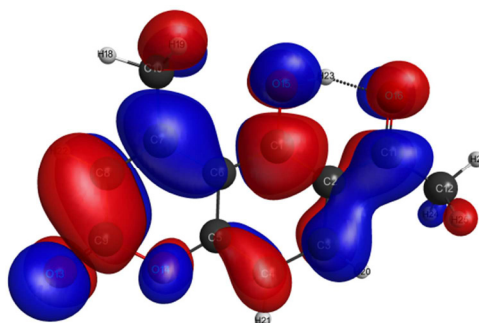
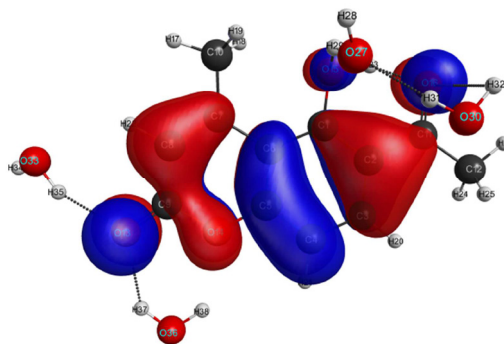


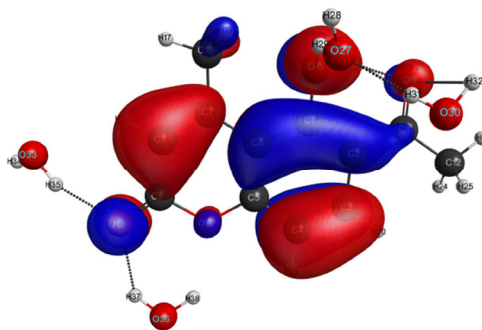
**Figure 4.** The molecular orbitals of LC molecule.

level by enforcing 6-31G(d,p) / B3LYP method. At ground state of LC / LCH molecules, an intra-molecular HB O15-H23.....O16 = C11 of length 1.569 / 1.520 Å and dihedral angle  $-0.3^\circ$  /  $4.2^\circ$  will be formed between hydroxyl and acetyl group. But, at the excited state, this intra-molecular HB is modified as O16-H23.....O15 = C1 of length 1.571 / 1.599 Å and

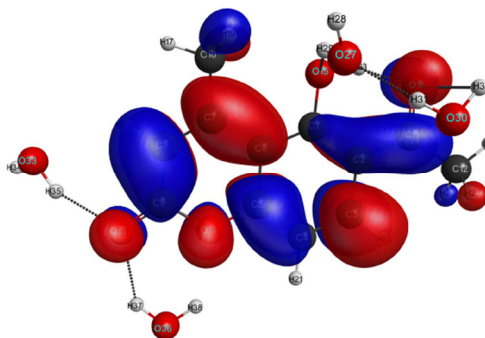
**Homo-1[-6.9933eV]**



**Homo[-6.6395eV]**



**Lumo[-2.0952eV]**



**Lumo+1[-1.8775eV]**

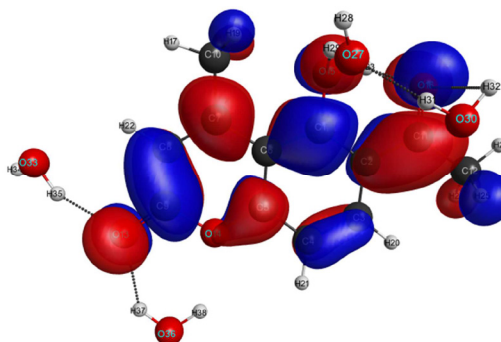


**Figure 5.** The molecular orbitals of LCH molecule.

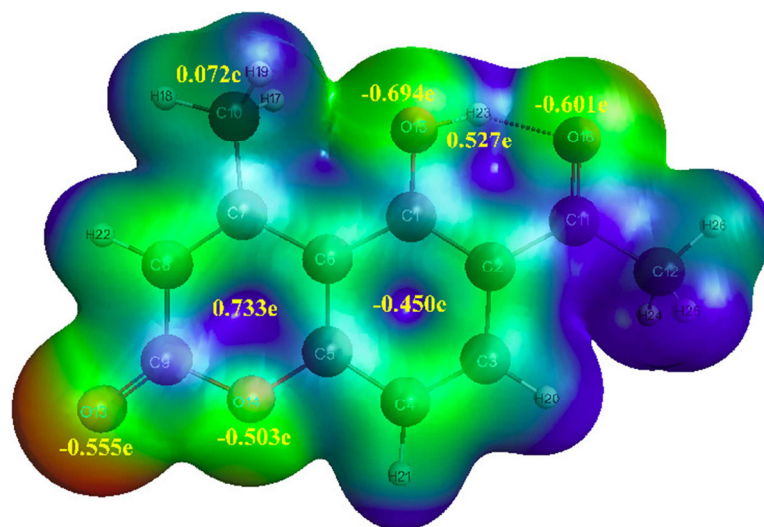
dihedral angle  $0.7^\circ / -10.6^\circ$ . In LCH molecule, four inter-molecular hydrogen bonds were formed; two were formed across 2-pyrone of the coumarin moiety, and another two inter-molecular hydrogen bonds formed between the hydroxyl group and acetyl group with one Hydrogen bond were formed between water molecules.

**Table 4.** Natural charges on different atoms of LC and LCH molecules at  $S_0$  and  $S_1$  states.

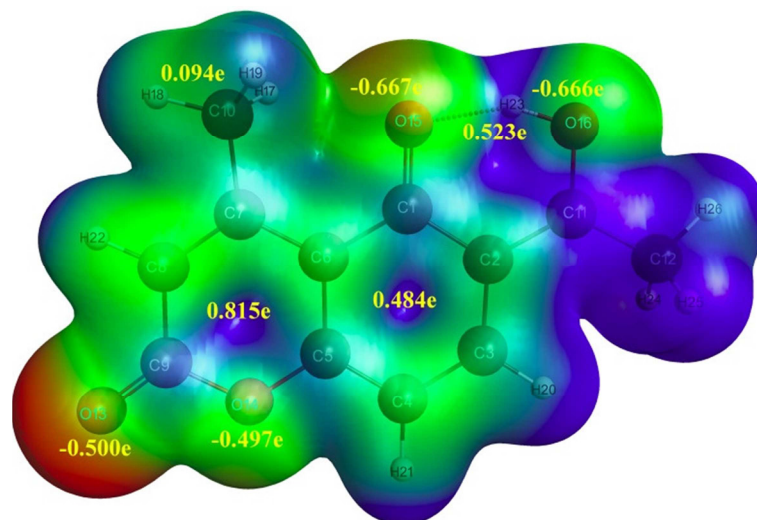
Atomic number	LC-S0	LC-S1	LCH-S0	LCH-S1
C1	0.4424	0.4534	0.4350	0.4554
C2	-0.2602	-0.2618	-0.2407	-0.2537
C3	-0.1677	-0.1094	-0.1549	-0.0926
C4	-0.3039	-0.3493	-0.3000	-0.3283
C5	0.4015	0.3888	0.3920	0.3721
C6	-0.1903	-0.1472	-0.1843	-0.1387
C7	0.0616	0.0823	0.0688	0.0861
C8	-0.3607	-0.2839	-0.3661	-0.2772
C9	0.7715	0.7520	0.7856	0.7671
C10	-0.7044	-0.7105	-0.7012	-0.7092
C11	0.5695	0.4078	0.6264	0.4264
C12	-0.7710	-0.7552	-0.7730	-0.7591
O13	-0.5557	-0.5003	-0.6337	-0.5749
O14	-0.5035	-0.4972	-0.5135	-0.5129
O15	-0.6941	-0.6670	-0.7363	-0.7160
O16	-0.6013	-0.6662	-0.6138	-0.6840
H17	0.2674	0.2834	0.2506	0.2466
H18	0.2423	0.2381	0.2697	0.2838
H19	0.2674	0.2831	0.2509	0.2745
H20	0.2480	0.2465	0.2536	0.2530
H21	0.2650	0.2634	0.2644	0.2653
H22	0.2609	0.2642	0.2943	0.3108
H23	0.5274	0.5233	0.5269	0.5217
H24	0.2580	0.2460	0.2510	0.2420
H25	0.2600	0.2470	0.2840	0.2750
H26	0.2700	0.2690	0.2650	0.2660

In the  $S_0$  state of LCH, inter-molecular hydrogen bonds like C9=O13.....H35-O33 / C9=O13.....H37-O36 formed across C9=O13 of coumarin moiety of their bond lengths 1.872 / 1.979Å and dihedral angles 19.2° / -0.2°. The other two inter-molecular hydrogen bonds like C1-O15.....H29-O27 / C11=O16.....H32-O30 formed across O15 and O16 of hydroxyl group and acetyl group of their bond lengths 1.935 / 2.675Å and dihedral angles 48.7° / -36°. Whereas, in the  $S_1$  state of LCH, inter-molecular hydrogen bonds like C9=O13.....H35-O33 / C9=O13.....H37-O36 formed across C9=O13 of coumarin moiety of their bond lengths 1.924 / 2.002Å and dihedral angles 9.2° / -1.5°. The other two inter-molecular hydrogen bonds like C1-O15.....H29-O27 / C11=O16.....H32-O30 formed across O15 and O16 of hydroxyl group and acetyl group of their bond lengths 1.865 / 2.070Å and dihedral angles 53.7° / -52.8°. One HB like O30-H31.....O27-H29 of length 1.814 / 1.843Å and dihedral angle 11.3° / 32.5° exist between two water molecules, which are bonded with hydroxyl group and acetyl group of LCH corresponds to  $S_0$  /  $S_1$  states.

In the first excited state of LC molecule, the charge on O15 / H23 decreased by 0.027e / 0.004e and the charge on O16 increased by 0.065e. While, in LCH molecule, the charge on O15 / H23 decreased by 0.020e / 0.005e and the charge on O16 increased by 0.07e. As the repercussion, the intra-molecular HB O15-H23.....O16=C11 is recasts as O16-H23.....O15=C1 due to transference of hydrogen atom H25 from hydroxyl group (O15-H23) to carbonyl group (C11-O16). Similarly, in the first excited state of LCH molecule, the inter-molecular HB's C9=O13.....H35-O33 / C9=O13.....H37-O36 elongated by 0.052 Å / 0.023Å due to decrease in charge on O13 and inter-molecular HB's C1-O15.....H29-O27 / C11=O16.....H32-O30 contracted by 0.070Å / 0.605Å due to decrease / increase in charge on O15 / O16 by 0.020e / 0.070e. The hydrogen bond



(a)



(b)

**Figure 6.** MEP with charges on different atoms and groups of LC molecule at (a)  $S_0$  and (b)  $S_1$  states.

O30-H31.....O27-H29 exists between water molecules gets elongated by 0.039 Å. The intra-molecular and inter-molecular HB lengths of pure and hydrated molecules at  $S_0$  and  $S_1$  states are tabulated in Tables 5,6.

### 3.7. PES scan and ESIHT mechanism

Envisaging and inspecting of PES curves is an efficient manner to investigate the ESIHT mechanism in LC and LCH molecules. Based on constrained relaxed and un-relaxed optimizations in both  $S_0$  and  $S_1$  states of LC and LCH molecules, potential energy curves have been scanned via intra-molecular HB O15-H23.....O16 = C1 by varying the O15-H23 and O16-H23 bond lengths from 0.8 to 1.8 Å in steps of 0.02 Å are presented in Figure 5. The ground and first excited state



potential energy scans of LC and LCH molecules can be done in gas phase with DFT/TDDFT methods by using hybrid functional B3LYP / 6-31G(d,p) basis set. The LC and LCH molecules can persist in unrelaxed first excited state ( $S_1^*$ ) by irradiating with the radiation of energy 3.73 eV and 3.88 eV, the O16-H23 bond extends to 1.535 Å and 1.425 Å respectively, the H23 atom isolated from O16 and embedded to O15. This is the junction at which ESIHT occurs. The LC and LCH molecules set in the relaxed first excited state  $S_1$  with O16-H23 bond length of 1.016Å and 1.008Å, respectively. The fluorescence may occur in both LC and LCH molecules with the emission of 2.40eV and 2.44eV energy; the molecules de-excited to unrelaxed ground state,  $S_0^*$ . At this condition, the O15-H23 bond length in LC and LCH molecules again elongates to 1.535Å and 1.71Å respectively, where the eviction of hydrogen atom (H23) from O15 to O16 occurs, and the molecules regress to their ground state. The hydrogen transfer mechanism in both LC and LCH molecules is professed by drawing potential energy surface scan maps, which are portrayed in Figures 8,9.

**Table 6.** Dihedral angles -A(°) across intra-molecular and inter-molecular HB's of LC and LCH at  $S_0$  and  $S_1$  states.

Hydrogen bonds	LC		LCH	
	$S_0$	$S_1$	$S_0$	$S_1$
$O_{15}-H_{23} \cdots O_{16} = C_{11} / O_{16}-H_{23} \cdots O_{15} = C_1$	-0.3	0.7	4.2	-10.6
$C_{11} = O_{16} \cdots H_{32} - O_{30}$	-	-	-36	-52.8
$C_1 = O_{15} \cdots H_{29} - O_{27}$	-	-	48.7	53.7
$C_9 = O_{13} \cdots H_{37} - O_{36}$	-	-	-0.2	-1.5
$C_9 = O_{13} \cdots H_{35} - O_{33}$	-	-	19.2	9.2
$O_{30}-H_{31} \cdots O_{27} - H_{29} (WB)$	-	-	11.3	32.5

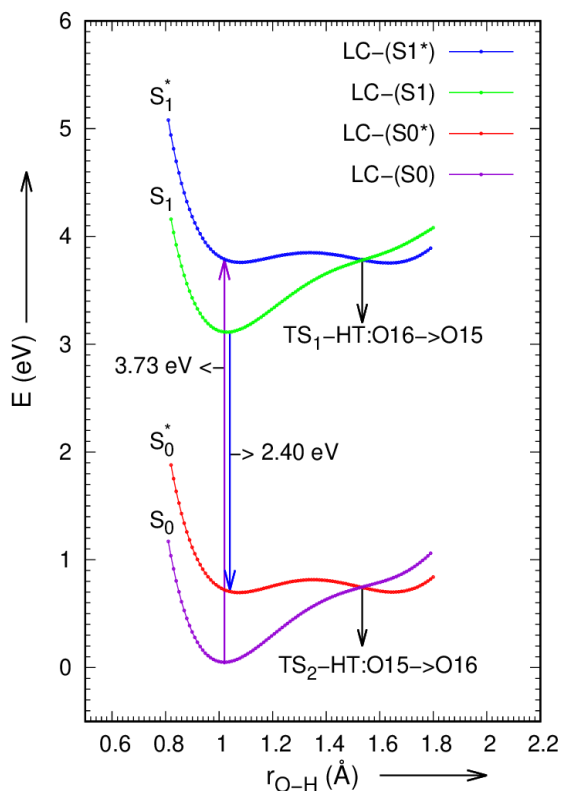


**Figure 8.** Potential energy plot along intra-molecular hydrogen transfer path in LC molecule.

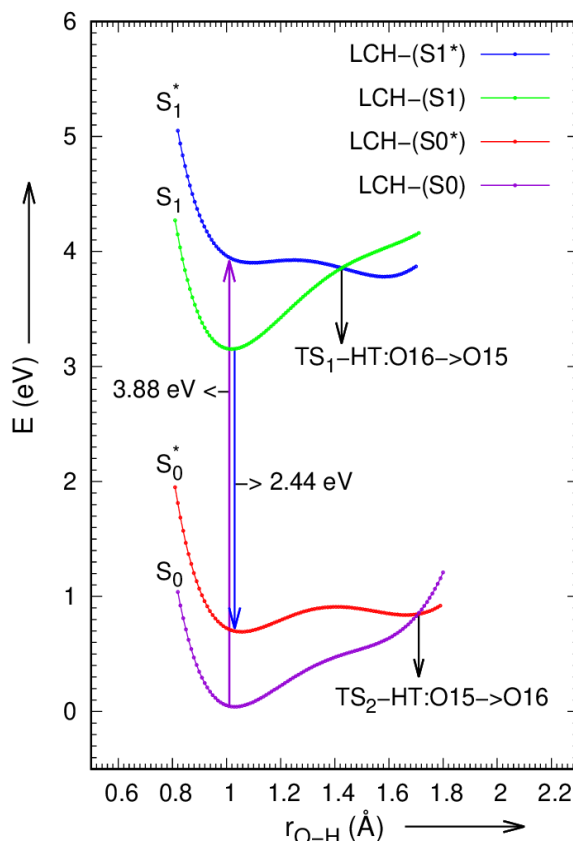


**Figure 9.** Potential energy plot along intra-molecular hydrogen transfer path in LCH molecule.

#### 4. Conclusion

The theoretical studies of LC and LCH molecules at  $S_0$  and  $S_1$  states using the DFT / TDDFT / EFP1 method proclaim the molecular structure, inter and intra-molecular HBs. The studies of frontier molecular orbitals and the NBO calculation both in the ground and excited states assist the leaning of hydrogen atom transpires from hydroxyl group to the acetyl group due to intramolecular charge allocation escalating the acidity / basicity of the donor-acceptor units. The detailed investigation of the UV-Vis spectra and energy specification along the hydrogen transfer track in an excited state asserts the ESIHT mechanism in LC and LCH molecules. To conclude, the relaxation dynamics of excited LC and LCH can be controlled by the intramolecular charge allocation and the hydrogen-bonding geometry in the  $S_1$  state. This computational study affords the existent research on the chemical and biological activity of the liqcoumarin molecule.

#### References

1. Miao M, Shi Y. Reconsideration on hydrogen bond strengthening or cleavage of photo-excited coumarin 102 in aqueous solvent: A DFT / TDDFT study. *Journal of Computational Chemistry* 2011; 32 (14): 3058-3061. doi: 10.1002/jcc.21888
2. Ramegowda M. Change in energy of hydrogen bonds upon excitation of 6-aminocoumarin: TDDFT / EFP1 study. *New Journal of Chemistry* 2013; 37: 2648-2653. doi: 10.1039/C3NJ00446E
3. Ramegowda M. A TDDFT/EFP1 study on hydrogen bonding dynamics of coumarin 151 in water. *Spectrochim Acta A* 2015; 137: 99-104. doi: 10.1016/j.saa.2014.08.017
4. Zhang M, Ren B, Wang Y, Zhao C. A DFT/TDDFT study on the excited hydrogen bonding dynamics in water solution. *Spectrochimica Acta Part A* 2013; 101: 191-195. doi: 10.1016/j.saa.2012.09.045
5. Li H, Pomelli CS, Jensen JH. Continuum solvation of large molecules described by QM/MM: a semi-iterative implementation of the PCM/EFP interface. *Theoret. Chimica Acta* 2003; 109: 71-84. doi: 10.1007/s00214-002-0427-x

6. Fedorov DG, Kitaura K, Li H, Jensen JH, Gorden MS. The polarizable continuum model interfaced with the Fragment Molecular Orbital method. *Journal of Computational Chemistry* 2006; 27: 976-985. doi: 10.1002/jcc.20406
7. Ramu YL, Jagadeesha K, Shivalingaswamy T, Ramegowda M. Microsolvation, hydrogen bond dynamics and excited state hydrogen atom transfer mechanism of 2,4'-dihydroxy chalcone. *Chemical Physics Letters* 2020; 739: 1-5. doi: 10.1016/j.cplett.2019.137030
8. Sardari S, Mori Y, Horita K, Micetich RG, Nishibe S, Danesh-talab M. Synthesis and antifungal activity of coumarins and angular furano-coumarins. *Bioorganic & Medicinal Chemistry Letters* 1999; 7: 1933. doi: 10.3390/molecules 22101672
9. Savarese M, Netti PA, Adamo C, Rega N, Ciofini I. Exploring the metric of excited state proton transfer reactions. *The Journal of Physical Chemistry B* 2013; 117: 16165. doi: 10.1021/jp507425x
10. Jagadeesha K, Ramu YL, Ramegowda M, Lokanath NK. Excited state hydrogen atom transfer in micro-solvated dicoumarol: A TDDFT / EFP1 study. *Spectrochim. Acta A* 2019; 208: 325-330. doi: 10.1016/j.saa.2018.10.015
11. Parvaiz M, Hussain K, Khalid S, Hussain N, Iram N et al. A review: medicinal importance of *Glycyrrhiza glabra* L. (Fabaceae Family). *Global Journal of Pharmacology* 2014; 8: 8-13. doi: 10.5829/idosi.gjp.2014.8.1.81179
12. Altay V, Karahan F, Öztürk M, Hakeem KR, Ilhan E et al. Molecular and ecological investigations on the wild populations of *Glycyrrhiza* L. taxa distributed in the East Mediterranean Area of Turkey. *Journal of Plant Research* 2016; 129: 1021-1032. doi: 10.1007/s10265-016-0864-6
13. Gupta KK, Taneja SC, Ahar KL, Atal CK. Flavonoids of *andropharis paniculata*. *Phytochemistry* 1983; 22: 314-315. doi: 10.1016/S0031-9422(00)80122-3
14. Williamson EM. *Potter's cyclopedia of herbal medicine*. C.W. Daniel, Saffron Walden, pp 269-271. 2003. doi: 10.1211/002235704322728111
15. Kinoshita T, Tamura Y, Mizutani K. The isolation and structure elucidation of minor isoflavonoids from licorice of *Glycyrrhiza glabra* origin. *Chemical and Pharmaceutical Bulletin* 2005; 53: 847-849. doi: 10.1248/cpb.53.847
16. Isbrucker RA, Burdock GA. Risk and safety assessment on the consumption of Licoriceroot (*Glycyrrhiza* sp.), its extract and powder as a food ingredient, with emphasis on the pharmacology and toxicology of glycyrrhizin. *Regul Toxicol Pharmacol* 2006; 46 (3): 167-192. doi: 10.1016/j.yrtph.2006.06.002
17. Patil SM, Patil MB, Sapkale GN. Antimicrobial activity of *Glycyrrhiza glabra* Linn. Roots. *International Journal of Chemical Sciences* 2009; 7 (1): 585-591. doi: 10.11648/j.plant.20170504.12
18. Satomi Y, Nishino H, Shibata S. Glycyrrhetic acid and related compounds induce G1 arrest and apoptosis in human hepatocellular carcinoma HepG2. *Anticancer Research* 2005; (6): 4043-4047.
19. Vaya J, Belinky PA, Aviram M. Structural aspects of the inhibitory effect of glabridin on LDL oxidation. *Free Radical Biology and Medicine* 1998; 24: 1419-1429. doi: 10.1016/s0891-5849(98)00006-9
20. Hossain MS, Hossain MA, Islam R, Alam AH, Zahan K et al. Antimicrobial and cytotoxic activities of 2-aminobenzoic acid and 2-aminophenol and their coordination complexes with Magnesium (Mg-II). *Pakistan Journal of Biological Sciences* 2004; 7: 25-27. doi: 10.4103/0253-7613.40489
21. Kakegawa H, Matsumoto H, Satoh T. Inhibitory effects of some natural products on the activation of hyaluronidase and their anti-allergic actions. *Chemical and Pharmaceutical Bulletin* 1992; 40: 1439-1442. doi: 10.1248/cpb.40.1439
22. Fujisawa Y, Sakamoto M, Matsushita M, Fujita T, Nishioka K. Glycyrrhizin inhibits the lytic pathway of complement-possible mechanism of its anti-inflammatory effect on liver cells in viral hepatitis. *Microbiology and Immunology* 2000; 44: 799-80. doi: 10.1055/s-0035-1557893
23. Cinatl J, Morgenstern B, Bauer G, Chandra P, Rabenau H et al. Glycyrrhizin, an active component of liquorice roots, and replication of SARS-associated coronavirus. *Lancet* 2003; 361: 2045-2046. doi: 10.1016/s0140-6736(03)13615-x
24. Srivastav VK, Tiwari M, Zhang X, Yao J. Synthesis and Antiretroviral Activity of 6-Acetyl-coumarin Derivatives against HIV-1 Infection. *Indian Journal of Pharmaceutical Sciences* 2018; 108-117. doi: 10.4172/pharmaceutical-sciences.1000335
25. Gajanan W, Rahul A, Neha K, Ravi R, Naveen KK et al. Synthesis of novel a-pyrano-chalcones and pyrazoline derivatives as *Plasmodium falciparum* growth inhibitors. *Bioorganic & Medicinal Chemistry Letters* 2010; 20: 4675-4678. doi: 10.1016/j.bmcl.2010.05.069
26. Hanwell MD, Curtis DE, Lonie DC, Vandermeersch T, Zurek E et al. Avogadro: An advanced semantic chemical editor, visualization and analysis platform. *Australian Journal of Chemistry* 2012; 4: 17. doi: 10.1186/1758-2946-4-17
27. Thomas AH, MMFFVI- MMFF94s Option for Energy Minimization Studies. *Journal of Computational Chemistry* 1999; 20 (7): 720-729. doi: 10.1002/(SICI)1096-987X(199905)20:7<720::AID-JCC7>3.0.CO;2-X
28. Schmidt MW, Baldrige KK, Boatz JA, Elbert ST, Gordon MS et al. General atomic and molecular electronic structure system. *Journal of Computational Chemistry* 1993; 14: 1347-1363. doi: 10.1002/jcc.540141112
29. Gordon MS, Schmidt MW. Advances in electronic structure theory: GAMESS a decade later. *Theory and Applications of Computational Chemistry* 2005; 1167-1189. doi: 10.1016/b978-044451719-7/50084-6

30. Dunning TH. Gaussian basis sets for use in correlated molecular calculations. I. The atoms boron through neon and hydrogen. *The Journal of Chemical Physics* 1989; 90: 1007-1023. doi: 10.1063/1.456153
31. Kohn W, Becke AD, Parr RG. Density Functional Theory of Electronic Structure. *The Journal of Physical Chemistry A* 1996; 100 (31) : 12974–12980. doi: 10.1021/jp960669l
32. Kim K, Jordan KD. Comparison of Density Functional and MP2 Calculations on the Water Monomer and Dimer. *The Journal of Physical Chemistry A* 1994; 98 (40): 10089–10094. doi: 10.1021/j100091A 24
33. Stephens PJ, Devlin FJ, Chabalowski CF, Frisch MJ. Ab initio calculation of vibrational absorption and circular dichroism spectra using density functional force fields. *The Journal of Physical Chemistry A* 1994 ; 98 (45): 11623-11627. doi: 10.1021/j100096A01
34. Stevens WH, Basch H, Krauss M, Jasien P. An effective fragment method for modeling solvent effects in quantummechanical calculations. *The Journal of Chemical Physics* 1996; 105: 1968. doi: 10.1063/1.472045
35. Cundari TR, Stevens WJ. Effective core potential methods for the lanthanides. *The Journal of Physical Chemistry* 1993; 98: 5555. doi: 10.1063/1.464902
36. Hay PJ, Wadt WR. Ab initio effective core potentials for molecular calculations. Potentials for the transition metal atoms Sc to Hg. *The Journal of Physical Chemistry* 1985; 82: 270. doi: 10.1063/1.448799
37. Tokura S, Sato T, Tsuneda T, Nakajima T, Hirao KJ. A dual-level state-specific time-dependent density-functional theory. *Journal of Computational Chemistry* 2008; 29 (8): 1187-97. doi: 10.1002/jcc.20871
38. Mahito C, Takao T, Kimihiko H. Excited state geometry optimizations by analytical energy gradient of long-range corrected time-dependent density functional theory. *The Journal of Chemical Physics* 2006; 124: 144106. doi: 10.1063/1.2186995.
39. Becke AD. Development and assessment of new exchange-correlation functionals *Journal of Chemical Physics* 1998; 109: 6264. doi: 10.1063/1.477267
40. Becke AD. Density-functional exchange-energy approximation with correct asymptotic behavior. *Physical Review A* 1998; 38: 3098. doi: 10.1103/PhysRevA.38.3098
41. Glendening ED, Landis CR, Weinhold F. Natural bond orbital methods. *Wiley Interdisciplinary Reviews: Computational Molecular Science* 2012; 2: 1-42. doi: 10.1002/wcms.51
42. Bode BM, Gordon MS. MacMolPlt: a graphical user interface for GAMESS. *Journal of Molecular Graphics and Modelling* 1998; 16 (3): 133-8. doi: 10.1016/s1093-3263(99) 00002-9
43. Bharadwaj KD, Ramaswamy M, Tiruvenkata RS, Rdhika S. Liqcoumarin- a novel coumarin from *Glycyrrhiza glabra*. *Phytochemistry* 1976; 15: 1182-1183.